A LINEAR CURVED-BEAM MODEL FOR THE ANALYSIS OF GALLOPING IN SUSPENDED CABLES

Angelo Luongo, Daniele Zulli and Giuseppe Piccardo

A LINEAR CURVED-BEAM MODEL FOR THE ANALYSIS OF GALLOPING IN SUSPENDED CABLES

ANGELO LUONGO, DANIELE ZULLI AND GIUSEPPE PICCARDO

A linear model of curved, prestressed, no-shear, elastic beam, loaded by wind forces, is formulated. The beam is assumed to be planar in its reference configuration, under its own weight and static wind forces. The incremental equilibrium equations around the prestressed state are derived, in which shear forces are condensed. By using a linear elastic constitutive law and accounting for damping and inertial effects, the complete equations of motion are obtained. They are then greatly simplified by estimating the order of magnitude of all their terms, under the hypotheses of small sag-to-span ratio, order-1 aspect ratio of the (compact) section, characteristic section radius much smaller than length (slender cable), small transversal-to-longitudinal and transversal-to-torsional wave velocity ratios. A system of two integrodifferential equations is drawn in the two transversal displacements only. A simplified model of aerodynamic forces is then developed according to a quasisteady formulation. The nonlinear, nontrivial equilibrium path of the cable subjected to increasing static wind forces is successively evaluated, and the influence of the angle of twist on the equilibrium is discussed. Then stability is studied by discretizing the equations of motion via a Galerkin approach and analyzing the small oscillations around the nontrivial equilibrium. Finally, the role of the angle of twist on the dynamic stability of the cable is discussed for some sample cables.

1. Introduction

The analysis of galloping oscillations of iced cables requires a careful formulation both of the mechanical model and of the aeroelastic forces, especially concerning nonlinear regimes [Luongo and Piccardo 1998]. The forces are usually modeled referring to the quasisteady theory, and they depend on the mean wind speed and on the angle of attack, which in turn depends on the velocity of the structure and on its surrounding flow. The structure is generally modeled as a perfectly flexible cable, that is as a one-dimensional continuum capable of translational displacements only [Luongo et al. 1984; Lee and Perkins 1992]. This assumption is reliable, since the torsion stiffness of the single cable is usually high and the bending stiffness is negligible, compared to the geometric one, because of the slenderness of the structure. However, simplified models of cables have highlighted the importance of the twist angle on the determination of aerodynamic forces and, therefore, on the dynamical behavior of the system. In particular, although Yu et al. [1993a], McConnel and Chang [1986], and White et al. [1991] have considered a sophisticated constitutive law, based on experimental results, in which the axial stress and torque depend both on elongation and torsion, they have neglected the initial curvature of the cable; as a result, the moment equilibrium around the tangent to the cable is violated, since the bending moment

is not taken into account. In an earlier paper [Luongo and Piccardo 1996] we have tried to correct the classic model, adding an energy of pure torsion to the elastic potential energy of the flexible cable, still ignoring every term of mechanical coupling. Therefore, the formulation of a consistent cable-beam model is a matter of great interest, able to take into account all the stiffnesses involved in the problem. To the best of our knowledge, similar models are usually employed in fully numerical approaches — see for instance [Diana et al. 1998] in the linear field, or [Lu and Perkins 1994] in somewhat different nonlinear problems — but they are not yet employed in semi-analytical analysis, like the one proposed here. A first approach to the subject was presented in [Luongo et al. 2005].

In this paper a linear model of curved elastic prestressed beam, subjected to aerodynamic forces induced by wind, is formulated. By taking into account the high slenderness of the body, the model is remarkably simplified via an analysis of the magnitude orders of all terms in the equations of motion. As a major result, it is shown that, at the leading order, the dynamic behavior of the cable is governed by the same equations as the perfectly flexible model in which, however, the positional and velocity-dependent forces also depend on the angle of twist, which is an integral function of the transversal displacements. In other words, the twist is a *passive variable*, slave to the normal and binormal translations. The reduced model thus obtained permits one to investigate the critical aeroelastic behavior of the cable, by highlighting the role of torsion on the stability of the structure.

The paper is organized as follows. The complete equations of motion are derived in Section 2 under the hypothesis of no-shear deformation of the beam. In Section 3 a reduced model is drawn from the complete one by neglecting small terms and statically condensing the tangent displacement and the angle of twist; therefore, two integrodifferential equations are obtained, in the transversal displacements only. In Section 4 an approximate model for the aerodynamic forces acting on the cable is developed, consistent with the approximations introduced. In Section 5 the nontrivial equilibrium path of the cable subjected to static wind forces is evaluated, and bifurcations causing galloping (Hopf bifurcations) are detected. Numerical results are discussed in Section 6, and some conclusions are drawn in Section 7.

2. Mechanical model

The cable is modeled as a beam constituted by a flexible centerline and rigid cross-sections. It is assumed that the cable, under its self-weight and the static component of the wind forces, takes a planar equilibrium configuration $\bar{\mathscr{C}}$ at time $t = 0$, which is selected as the reference configuration. The linear equations of motion governing the small oscillations around such equilibrium position are sought.

Let $\bar{\mathbf{x}} = \bar{\mathbf{x}}(s)$ be the parametric equation of the centerline in $\bar{\mathscr{C}}$, where $\bar{\mathbf{x}}$ is the position vector and $s \in [0, \ell]$ is a curvilinear abscissa. It is supposed that the inertia principal axes of the section coincide in $\bar{\mathscr{C}}$ with the Frenet triad $\bar{\boldsymbol{\beta}}(s) := \{\bar{\mathbf{a}}_1(s), \bar{\mathbf{a}}_2(s), \bar{\mathbf{a}}_3(s)\}$, where $\bar{\mathbf{a}}_1 \equiv \bar{\mathbf{x}}'$ (with $' = d/ds$) is the unit vector tangent to the curve, $\bar{\mathbf{a}}_2$ is the normal and $\bar{\mathbf{a}}_3$ the binormal (Figure 1, left). According to the Frenet formulas, it follows that $\bar{\mathbf{a}}_1' = \bar{\kappa}\bar{\mathbf{a}}_2$, $\bar{\mathbf{a}}_2' = -\bar{\kappa}\bar{\mathbf{a}}_1$, $\bar{\mathbf{a}}_3' = \mathbf{0}$, where $\bar{\kappa} = \bar{\kappa}(s)$ is the modulus of the curvature vector $\bar{\boldsymbol{\kappa}} = \bar{\kappa}\bar{\mathbf{a}}_3$ in $\bar{\mathscr{C}}$.

Now consider an adjacent configuration $\mathscr{C}$, assumed by the cable at the time $t > 0$. Denoting by $\mathbf{u}(s, t)$ and $\boldsymbol{\vartheta}(s, t)$ the translation of the centerline and the (infinitesimal) rotation of the cross-section at abscissa s, respectively, the position vector $\mathbf{x}(s, t)$ and the attitude of the inertia principal triad $\boldsymbol{\beta} :=$
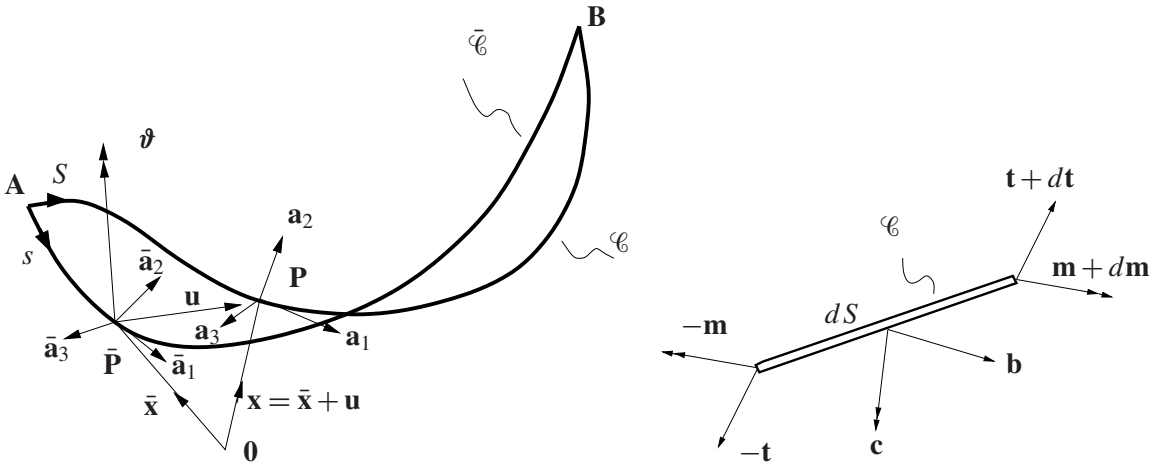
Figure 1. Left: configurations of the cable. Right: forces and couples on an infinitesimal element.

$\{\mathbf{a}_1(s, t), \mathbf{a}_2(s, t), \mathbf{a}_3(s, t)\}$ in $\mathscr{C}$ are given by (see Figure 1, left):

$$\mathbf{x} = \bar{\mathbf{x}} + \mathbf{u}, \qquad \mathbf{a}_i = \bar{\mathbf{a}}_i + \boldsymbol{\vartheta} \times \bar{\mathbf{a}}_i \quad \text{for } i = 1, 2, 3. \tag{1}$$

The slenderness of the beam suggests one may neglect the shear deformation; therefore the cross-sections are assumed to remain orthogonal to the centerline in any configuration. This internal constraint is expressed by the condition $\mathbf{x}' = (1 + \varepsilon)\mathbf{a}_1$, $\mathbf{a}_1$ being normal to the section and $d\mathbf{x}/dS = \mathbf{x}'/(1 + \varepsilon)$ the unit vector tangent to the strained centerline at the actual abscissa $S = S(s)$, with $\varepsilon := dS/ds - 1$ the *unit extension*. By letting $\mathbf{u} = u\mathbf{a}_1 + v\mathbf{a}_2 + w\mathbf{a}_3$ and $\boldsymbol{\vartheta} = \vartheta_1\mathbf{a}_1 + \vartheta_2\mathbf{a}_2 + \vartheta_3\mathbf{a}_3$, and taking into account that $\varepsilon \ll 1$, it follows that

$$\vartheta_2 = -w', \quad \vartheta_3 = v' + \bar{\kappa}u \tag{2}$$

and

$$\varepsilon = u' - \bar{\kappa}v.$$

Due to the constraints (2), the configuration variables $u, v, w, \vartheta_1, \vartheta_2, \vartheta_3$ are reduced to the three translation components and the unique rotation component $\vartheta := \vartheta_1$, called the *twist angle*.

Finally, by defining the incremental curvature vector $\boldsymbol{\kappa} := \partial\boldsymbol{\vartheta}/\partial s$, using (2) and projecting on $\bar{\boldsymbol{\beta}}$, the torsion κ_1 and the bendings κ_2 and κ_3 are found to be

$$\kappa_1 = \vartheta' + \bar{\kappa}w', \quad \kappa_2 = -w'' + \bar{\kappa}\vartheta, \quad \kappa_3 = v'' + (\bar{\kappa}u)'. \tag{3}$$

We next derive the equilibrium equations. By considering an infinitesimal cable element in the actual configuration (Figure 1, right), and denoting by $\mathbf{t}(s, t)$ and $\mathbf{m}(s, t)$ the internal contact force and couple, respectively, acting at abscissa s at time t, the balance equations become, in Lagrangian form,

$$\mathbf{t}' + \mathbf{b} = \mathbf{0}, \quad \mathbf{m}' + \mathbf{x}' \times \mathbf{t} + \mathbf{c} = \mathbf{0}, \tag{4}$$

where $\mathbf{b} := \mathbf{b}(s, t)$ and $\mathbf{c} := \mathbf{c}(s, t)$ are the body force and couple densities per undeformed arc-length, including inertial and damping effects. It is assumed that in the planar reference configuration $\bar{\mathscr{C}}$ the

cable is loaded by body forces $\bar{\mathbf{b}}(s)$ and no couples: $\bar{\mathbf{c}}(s) \equiv \mathbf{0}$. By neglecting flexural effects in its own plane, the cable is stressed in $\bar{\mathcal{C}}$ exclusively by axial forces, namely $\bar{\mathbf{t}} = \bar{T}\bar{\mathbf{a}}_1$ and $\bar{\mathbf{m}} = \mathbf{0}$, with $\bar{\mathbf{t}}' + \bar{\mathbf{b}} = \mathbf{0}$. By subtracting this latter from $(4)_1$, we obtain *incremental equilibrium equations*

$$(\mathbf{t}' - \bar{\mathbf{t}}') + \hat{\mathbf{b}} = \mathbf{0}, \quad \mathbf{m}' + \mathbf{x}' \times \mathbf{t} + \hat{\mathbf{c}} = \mathbf{0},$$

with $\hat{\mathbf{b}} := \mathbf{b} - \bar{\mathbf{b}}$ and $\hat{\mathbf{c}} := \mathbf{c} - \bar{\mathbf{c}}$. By letting $\mathbf{t} = (\bar{T} + \hat{T}_1)\mathbf{a}_1 + \hat{T}_2\mathbf{a}_2 + \hat{T}_3\mathbf{a}_3$, $\mathbf{m} = \hat{M}_1\mathbf{a}_1 + \hat{M}_2\mathbf{a}_2 + \hat{M}_3\mathbf{a}_3$, using (1) and projecting onto $\bar{\boldsymbol{\beta}}$, six scalar equations follow. After linearization in the incremental quantities and condensation of the reactive stresses $\hat{T}_2$ and $\hat{T}_3$, the following four equilibrium equations are obtained in the active stresses $\hat{T}_1, \hat{M}_1, \hat{M}_2, \hat{M}_3$ (hats omitted):

$$
\begin{aligned}
T_1' - \bar{T}\bar{\kappa}(v' + \bar{\kappa}u) + M_3'\bar{\kappa} + \tilde{b}_1 &= 0, \\
-M_3'' + \left(\bar{T}(v' + \bar{\kappa}u)\right)' + T_1\bar{\kappa} + \tilde{b}_2 &= 0, \\
M_2'' + (M_1\bar{\kappa})' + (\bar{T}w')' + \tilde{b}_3 &= 0, \\
M_1' - M_2\bar{\kappa} + c_1 &= 0,
\end{aligned}
\tag{5}
$$

where

$$\tilde{b}_1 := b_1 + \bar{\kappa}c_3, \quad \tilde{b}_2 := b_2 - c_3', \quad \tilde{b}_3 := b_3 + c_2'.$$

Finally, a linear, uncoupled, elastic law is assumed between the incremental active stress and strain components:

$$T_1 = EA\varepsilon, \quad M_1 = GJ\kappa_1, \quad M_2 = EI_2\kappa_2, \quad M_3 = EI_3\kappa_3, \tag{6}$$

in which EA, GJ, EI_2 and EI_3 are the axial, torsional and flexural stiffnesses of the cable and hats have been dropped. In view of (6), the equations of motion (5) become

$$
\begin{aligned}
EA(u' - \bar{\kappa}v)' + EI_3\bar{\kappa}\left(v'' + (\bar{\kappa}u)'\right)' - \bar{T}\bar{\kappa}(v' + \bar{\kappa}u) + \tilde{b}_{a_1} - c_u\dot{u} - m\ddot{u} &= 0, \\
EA\bar{\kappa}(u' - \bar{\kappa}v) - EI_3\left(v'' + (\bar{\kappa}u)'\right)'' + \left(\bar{T}(v' + \bar{\kappa}u)\right)' + \tilde{b}_{a_2} - c_v\dot{v} - m\ddot{v} &= 0, \\
EI_2(-w'' + \bar{\kappa}\vartheta)'' + GJ\left(\bar{\kappa}(\bar{\kappa}w' + \vartheta')\right)' + (\bar{T}w')' + \tilde{b}_{a_3} - c_w\dot{w} - m\ddot{w} &= 0, \\
GJ(\bar{\kappa}w' + \vartheta')' - EI_2\bar{\kappa}(-w'' + \bar{\kappa}\vartheta) + c_{a_1} - c_\vartheta\dot{\vartheta} - \mathcal{J}_1\ddot{\vartheta} &= 0,
\end{aligned}
\tag{7}
$$

where the body forces $\tilde{b}_i$ and couple c_1 have been expressed as the sum of aerodynamic (index a), damping and inertia effects, $c_u, c_v, c_w, c_\vartheta$ being structural damping coefficients, m the mass linear density and $\mathcal{J}_1$ the inertia polar moment of the section. It is worth noting that Equations (7) are block-uncoupled; that is, the in-plane oscillations of the cable are independent of out-of-plane oscillations, the latter involving torsion. However, if the forces $\tilde{b}_i$ depend on the configuration variables, as occurs for the aerodynamic forces, the equations are coupled.

Equations (7) must be accompanied by suitable boundary conditions. If the cable is restrained at both ends by spherical hinges, the displacements and moments must vanish there:

$$
\left.
\begin{aligned}
u &= 0, & GJ(\vartheta' + \bar{\kappa}w') &= 0, \\
v &= 0, & EI_2(-w'' + \bar{\kappa}\vartheta) &= 0, \\
w &= 0, & EI_3\left(v'' + (\bar{\kappa}u)'\right) &= 0,
\end{aligned}
\right\} \quad \text{at } s = 0, \ell. \tag{8}
$$

The problem is completed by the initial conditions; here it is assumed that the body is at rest at $t = 0$.

3. Reduced equations of motion

The equations of motion previously obtained are too complicated to be treated analytically; therefore, a simplified model is developed in this Section. First, the classical hypothesis of small sag-to-span ratio d/ℓ is introduced [Luongo et al. 1984; Lee and Perkins 1992; Irvine and Caughey 1984], commonly accepted for cables falling into the technical range. Then, advantage is drawn from the fact that the cable is a very slender body; hence, the flexural-torsional effects are expected to be smaller than the funicular effects, except close to the boundaries. On the other hand, bending effects cannot be completely neglected, since, due to the (small but finite) initial curvature, the bending moment contributes to the moment equilibrium around the tangent to the cable.

3.1. *Order-of-magnitude analysis.* According to the previous ideas, we perform an order-of-magnitude analysis of all the terms in the equations of motion (7) and boundary conditions (8). First, equations (7) and (8) are written in a nondimensional form. We set

$$s^* = \frac{s}{\ell}, \quad \omega = \frac{\pi}{\ell}\sqrt{\frac{\bar{T}}{m}}, \quad t^* = \omega t, \quad u^* = \frac{u}{\ell}, \quad v^* = \frac{v}{\ell}, \quad w^* = \frac{w}{\ell}, \quad \vartheta^* = \vartheta, \tag{9}$$

$$c_\alpha^* = \frac{\omega \ell^2}{EA} c_\alpha, \quad c_\vartheta^* = \frac{\omega}{EA} c_\vartheta, \quad m^* = \frac{\omega^2 \ell^2}{EA} m, \quad \mathcal{J}_1^* = \frac{\omega^2}{EA} \mathcal{J}_1, \quad b_{a_i}^* = \frac{\ell}{EA} \tilde{b}_{a_i}, \quad c_{a_1}^* = \frac{\tilde{c}_{a_1}}{EA}, \quad \kappa^* = \bar{\kappa}\ell,$$

where α assumes the values u, v, w, and we introduce the nondimensional quantities

$$\delta = \frac{8d}{\ell}, \quad \tau = \frac{\bar{T}}{EA}, \quad \varrho = \frac{r}{\ell}, \quad \beta = \frac{GJ}{EI}. \tag{10}$$

The equations then become

$$(u' - \kappa v)' + \varrho^2 \kappa (v'' + (\kappa u)')' - \tau\kappa(v' + \kappa u) + b_{a_1} - c_u \dot{u} - m\ddot{u} = 0,$$
$$\kappa(u' - \kappa v) - \varrho^2 (v'' + (\kappa u)')'' + (\tau(v' + \kappa u))' + b_{a_2} - c_v \dot{v} - m\ddot{v} = 0,$$
$$\varrho^2(-w'' + \kappa\vartheta)'' + \varrho^2 \beta(\kappa(\kappa w' + \vartheta'))' + (\tau w')' + b_{a_3} - c_w \dot{w} - m\ddot{w} = 0,$$
$$\beta\varrho^2(\kappa w' + \vartheta')' - \varrho^2 \kappa(-w'' + \kappa\vartheta) + c_{a_1} - c_\vartheta \dot{\vartheta} - \mathcal{J}_1 \ddot{\vartheta} = 0,$$

$$\tag{11}$$

together with

$$\left.\begin{aligned} u = 0, \quad & \beta\varrho^2(\vartheta' + \kappa w') = 0, \\ v = 0, \quad & \varrho^2(-w'' + \kappa\vartheta) = 0, \\ w = 0, \quad & \varrho^2(v'' + (\kappa u)') = 0 \end{aligned}\right\} \quad \text{at } s = 0, 1. \tag{12}$$

where the star has been omitted for the sake of simplicity, the dot stands for differentiation with respect to t^* and the prime stands for differentiation with respect to s^*. In (10), δ is the nondimensional sag, τ the nondimensional prestress, ϱ the nondimensional inertia radius $r = \sqrt{I/A}$ of the section, assumed to be circular ($I_2 = I_3 \equiv I$), and β the nondimensional torsional stiffness. For a commonly employed overhead transmission line, $\delta = \mathbb{O}(10^{-1})$, $\tau \leq \mathbb{O}(\delta^3)$ and $\varrho \leq \mathbb{O}(\delta^3)$, while $\beta = \mathbb{O}(1)$. Moreover, from the catenary theory, it is well known that $\tau(s) = \tau(1/2) + \delta^2 f(s)$ and $\kappa(s) = \delta + \delta^2 g(s)$, with $\mathbb{O}(f(s)) = 1$, $\mathbb{O}(g(s)) = 1$. Therefore, according to parabolic cable theory (see [Irvine and Caughey 1984]), we can

consider, with an error of second order in δ,

$$\tau(s) = \text{const}, \quad \kappa(s) = \text{const}.$$

Next we must estimate the order of magnitude of the displacement component ratios. We assume that

$$\mathbb{O}\left(\frac{u}{v}\right) = \delta, \quad \mathbb{O}\left(\frac{\vartheta}{w}\right) = \frac{1}{\delta}, \quad \mathbb{O}\left(\frac{v}{w}\right) = 1, \tag{13}$$

together with

$$\frac{\partial^n u}{\partial s^n} = \mathbb{O}(u), \quad \frac{\partial^n v}{\partial s^n} = \mathbb{O}(v), \quad \frac{\partial^n w}{\partial s^n} = \mathbb{O}(w), \quad n = 1, 2, \dots \tag{14}$$

and

$$\frac{\partial \vartheta}{\partial s} = \mathbb{O}(w\delta), \quad \frac{\partial^2 \vartheta}{\partial s^2} = \mathbb{O}(w\delta). \tag{15}$$

Equation $(13)_1$ is suggested by the linear theory [Irvine and Caughey 1984], and by the fact that $u \to 0$ in the (prevalently) transversal motions ($v \gg u$) when $\delta \to 0$. Equations (14) also follow from the linear theory, when the trigonometric nature of the eigenfunctions is recognized. Estimates $(13)_2$ and (15) are instead drawn by inspection of the solution of the linearized Equation $(11)_4$ and the relevant boundary conditions (see Appendix A). Equation $(13)_3$ is self-explanatory. It is worth noting that, due to the different boundary conditions, the translations u, v and w must vanish at the ends, and therefore they are *fast-varying functions in space* (that is, their dimensional counterparts vary on a scale of typical length ℓ), whereas the twist angle ϑ, being different from zero at the ends, can vary in a much slower manner (that is, on a scale of much larger typical length). As illustrated in detail in Appendix A, ϑ is indeed a *slow-varying function* (in space) in symmetrical modes (in which $\vartheta = \mathbb{O}(w/\delta)$), and again a fast-varying function in antisymmetrical modes (in which $\vartheta = \mathbb{O}(w\delta)$). The upper estimate of ϑ has been adopted for all motions, in order to account also for nonsymmetrical modes of cables supported at different levels.

By using previous the estimates in (11) and (12) and retaining only the dominant terms, we obtain a set of *reduced equations*. Returning to dimensional form, they read

$$EA\left(u' - \bar{\kappa}v\right)' + b_{a_1} - c_u \dot{u} - m\ddot{u} = 0,$$
$$EA\bar{\kappa}(u' - \bar{\kappa}v) + \bar{T}v'' + b_{a_2} - c_v \dot{v} - m\ddot{v} = 0,$$
$$\bar{T}w'' + b_{a_3} - c_w \dot{w} - m\ddot{w} = 0, \tag{16}$$
$$GJ\vartheta'' - EI\bar{\kappa}^2\vartheta + (EI + GJ)\bar{\kappa}w'' + c_{a_1} - c_\vartheta \dot{\vartheta} - \mathscr{J}_1 \ddot{\vartheta} = 0,$$

with boundary conditions

$$u = 0, \quad v = 0, \quad w = 0, \quad GJ(\vartheta' + \bar{\kappa}w') = 0 \quad \text{at } s = 0, \ell. \tag{17}$$

The first three equations in (16) are identical to those of the flexible cable [Lee and Perkins 1992]. The fourth (16) is also known in the literature, since it represents the moment equilibrium around the tangent of a planar circular arch [Lee and Chao 2000]. It follows directly from Equations (3), $(5)_4$ and (6), since all its terms, being of the same order, were retained in the analysis. In spite of this apparently simplistic result, and as a major finding of this paper, Equations (16) prove that the perfectly flexible

cable and the twisting of a circular arch are *consistent models*. In other words, neglecting bending effects in translational equilibrium, while retaining them in rotational equilibrium, does not entail ordering violation from an asymptotic point of view.

From (16) it follows that, if the body forces are independent of ϑ or even zero (as happens in free vibrations), the translational motion is independent of ϑ, which is therefore a *passive variable*, slave to translations; whereas, if the body forces depend on ϑ, as in the aerodynamic case, the twist angle does affect the dynamics of the body.

The reduced equations (16) inconsistently appear to be non-self-adjoint in the elastic part. Indeed, the symmetry of the differential operator has been destroyed by the neglecting of the term $(EI + GJ)\bar{\kappa}(\vartheta w')'$ in the out-of-plane equation of motion (16)$_3$, compared to the dominant term $\bar{T} w''$. However, this inconsistency turns out to be only of formal type, as has been checked numerically (see Section 6.1); it can easily be removed by reintroducing the small term.

Equations (16) are accompanied by the boundary conditions (17); equations expressing the vanishing of the bending moments have been ignored, consistently with the approximation adopted, which does not permit description of the boundary layers.

3.2. *Static condensation.* It is well known that, in the framework of parabolic cable theory, the tangential inertia force $-m\ddot{u}$ (and the damping force $c_u \dot{u}$) can be neglected in the prevalently transversal motions, since the longitudinal natural frequencies are much higher than the transversal ones (quasisteady stretching). This allows one to statically condense the tangent displacement u by expressing it as an integral of the transverse displacement v:

$$u(s, t) = \bar{\kappa} \left(\int_0^s v(\xi, t) d\xi - \frac{s}{\ell} \int_0^\ell v(\xi, t) d\xi \right), \tag{18}$$

where $b_{a_1} = 0$ has been considered for simplicity.

Here we apply an analogous procedure to the equation (16)$_4$ governing the twist. First, observe that the squared torsional frequencies of a single cable are much higher than the transversal ones. For example, for the commonly used strand cables, which are relatively soft in torsion, this ratio is of the order of 10^{-2} (a case study is discussed in Section 6). The inertia couple $-\mathcal{I}_1 \ddot{\vartheta}$ and the damping couple $c_\vartheta \dot{\vartheta}$ are neglected in (16)$_4$, and ϑ is obtained in integral form (quasisteady twisting). Taking $c_{a_1} = 0$ for simplicity, we obtain

$$\vartheta(s, t) = -\frac{GJ + EI}{\sqrt{GJ\, EI}} \int_0^s w''(\xi, t) \sinh\left[k(s - \xi)\right] d\xi + A \cosh ks + B \sinh ks, \tag{19}$$

where we have set $k := \bar{\kappa}\sqrt{EI/GJ}$ and the arbitrary constants A and B are determined by the boundary conditions in the second line of (8).

4. Aerodynamic forces

Modeling aerodynamic loads is a very difficult task, often handled in the literature under simplifying hypotheses. The most popular model adopted for the structure is the unbounded rigid cylinder; however, the iced cable problem adds further difficulties, due to the curvature of its centerline and the random

variation of the section. To tentatively tackle the problem, a simple model is adopted here, by introducing the following assumptions: (a) *quasisteady theory* [Blevins 1990] is believed applicable, according to which the loads acting on the moving body at a certain instant are identical to those exerted on the body at rest in the same position; (b) the curvature of the cable is negligibly small; (c) loads are evaluated in the current configuration $\mathcal{C}$, by accounting for the twist angle ϑ, but neglecting the smaller flexural rotations $\vartheta_{2,3} = \mathbb{O}(\vartheta\delta)$ (remember Equations (2) and (13)$_2$), which, according to the so-called *cosine rule* [Strømmen and Hjorth-Hansen 1995], have small influence; (d) the ice is assumed to be uniformly distributed along the cable, consistently with the hypothesis of planar reference configuration; (e) aerodynamic couples are neglected.

Now consider a wind flow of mean velocity $\mathbf{U} = U\mathbf{a}_z$, blowing horizontally and normally to the initial (no wind) planar configuration of the cable (Figure 2, left). Three different attitudes of the cross-section in its own plane are considered (Figure 2, right): (a) the initial configuration $\mathcal{C}_0$ (axes $\mathbf{a}_{2_0}$, $\mathbf{a}_{3_0} \equiv \mathbf{a}_z$), in which the cable is only subjected to gravity; (b) the reference configuration $\bar{\mathcal{C}}$ (axes $\bar{\mathbf{a}}_2$, $\bar{\mathbf{a}}_3$), in which the cable is also loaded by (uniform) static wind forces; (c) the actual configuration $\mathcal{C}$ (axes $\mathbf{a}_2$, $\mathbf{a}_3$), in which the cable is also loaded by (non uniform) dynamic wind forces. The twist angle caused by the static forces coincides, within small quantities of order $\mathbb{O}(\delta^2)$, with the angle of rotation φ experienced by the cable passing from $\mathcal{C}_0$ to $\bar{\mathcal{C}}$ (see Figure 2), which depends only on the mean wind velocity U. The twist angle ϑ caused by the dynamic forces depends, in addition to U, on the abscissa s and on time t. The angle φ is assumed to be large; the angle ϑ is assumed to be small.

According to quasisteady theory, the flow exerts the following aerodynamic force on the section:

$$\mathbf{b}_a = \tfrac{1}{2}\rho_a V r (c_d(\gamma)\mathbf{V} + c_l(\gamma)\mathbf{a}_1 \times \mathbf{V}), \qquad (20)$$
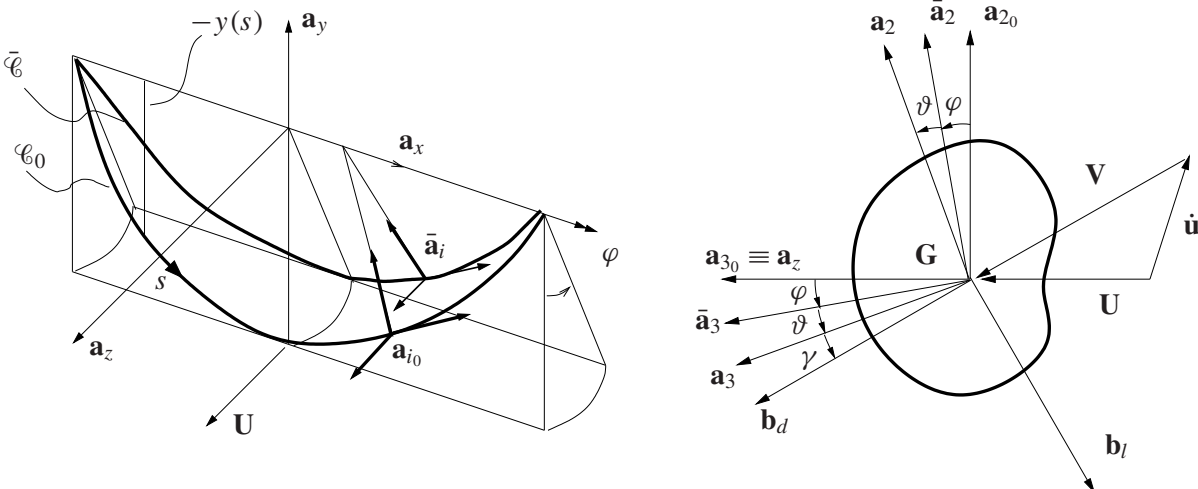

Figure 2. Aerodynamic forces. Left: cable configuration. Right: transversal section, mean wind velocity $\mathbf{U}$, relative wind velocity $\mathbf{V}$, angle of attack γ, drag force $\mathbf{b}_d$ and lift force $\mathbf{b}_l$.

where ρ_a is the air density, $\mathbf{V}$ is the relative velocity of the wind with respect to the section, $V = \|\mathbf{V}\|$ its modulus, and c_d and c_l two aerodynamic coefficients, called of *drag* and *lift*, respectively. These coefficients depend on the shape of the section and on the *angle of attack*,

$$\gamma := -\arcsin\left(\frac{\mathbf{V}}{V} \cdot \mathbf{a}_2\right), \tag{21}$$

that is, the angle between $\mathbf{V}$ and a reference material axis, taken as $\mathbf{a}_3$ here. The two components of $\mathbf{b}_a$, along-wind $\mathbf{b}_d$ and cross-wind $\mathbf{b}_l$, are usually known as drag and lift forces, respectively; see Figure 2, right.

Equations (20) and (21) allow one to evaluate the force $\mathbf{b}_a$ once the relative velocity $\mathbf{V}$ is known. If the section underwent only a translation, the relative velocity would be easily obtained as $\mathbf{V} = \mathbf{U} - \dot{v}\mathbf{a}_2 - \dot{w}\mathbf{a}_3$. In contrast, a nonvanishing twist velocity $\dot{\vartheta}$ entails some difficulties, since $\mathbf{V}$ becomes a function of the point $\mathbf{P}$ on the boundary. To overcome the problem, the notion of *characteristic radius* [Blevins 1990] has been introduced in the literature, which consists of selecting a special point $\mathbf{P}_c$ on the boundary of the section, in which to evaluate a "characteristic relative velocity" $\mathbf{V}_c$, to be attributed to all the points of the section. The problem at hand, however, is simpler. Indeed, the ratio between the velocity of *any* point of the boundary due to the twist and the velocity of the centerline is of the order $\mathbb{O}(\dot{\vartheta}r/\dot{w}) = \mathbb{O}(\dot{\vartheta}^*\varrho/\dot{w}^*)$. Since, by Equation (13)$_2$, $\mathbb{O}(\dot{\vartheta}^*/\dot{w}^*) \leq 1/\delta$, the previous contribution is at most of the order $\mathbb{O}(\varrho/\delta) = \mathbb{O}(\delta^2)$, and therefore it is negligible. Hence, *the twist velocity $\dot{\vartheta}$ has practically no effects on the aerodynamic forces of cables not having evanescent sag.* In contrast, the twist angle ϑ *does affect the forces via the angle of attack* γ; consequently $\mathbf{b}_a = \mathbf{b}_a(\vartheta, \dot{v}, \dot{w}; \varphi(U), U)$.

By letting $\mathbf{V} = \mathbf{U} - \dot{v}\mathbf{a}_2 - \dot{w}\mathbf{a}_3$ in (20) and (21) and linearizing these equations in $\dot{v}$, $\dot{w}$ and ϑ, we get

$$V = U\left(1 - \frac{\dot{v}}{U}\sin\varphi - \frac{\dot{w}}{U}\cos\varphi\right), \tag{22}$$

$$\gamma = -\varphi - \vartheta + \frac{\dot{v}}{U}\cos\varphi - \frac{\dot{w}}{U}\sin\varphi. \tag{23}$$

Equation (23) shows that when $\mathcal{C}$ approaches $\bar{\mathcal{C}}$, that is, when ϑ, $\dot{v}$, $\dot{w}$ approach zero, the angle γ approaches $-\varphi$. Hence, by expanding the aerodynamic coefficients $c_\alpha(\gamma)$ ($\alpha = d, l$) around $\gamma = -\varphi$, one has

$$c_\alpha(\gamma) = \bar{c}_\alpha + (\gamma + \varphi)\bar{c}'_\alpha + \tfrac{1}{2}(\gamma + \varphi)^2\bar{c}''_\alpha + \cdots, \qquad \alpha = d, l, \tag{24}$$

where $\bar{c}_\alpha$, $\bar{c}'_\alpha$, $\ldots$, are the values assumed by c_α and its derivatives at $\bar{\mathcal{C}}$. Finally, by substituting (22)–(24) into (20) and projecting this last equation onto the $\bar{\mathbf{a}}_2$ and $\bar{\mathbf{a}}_3$ axes, the following force components are derived:

$$\begin{aligned} b_{a_2} &= \bar{b}_{a_2}(\varphi) + c_{2\vartheta}(\varphi)\vartheta + c_{2v}(\varphi)\dot{v} + c_{2w}(\varphi)\dot{w}, \\ b_{a_3} &= \bar{b}_{a_3}(\varphi) + c_{3\vartheta}(\varphi)\vartheta + c_{3v}(\varphi)\dot{v} + c_{3w}(\varphi)\dot{w}. \end{aligned} \tag{25}$$

In these equations, the $\bar{b}_{a_i}$ are the static forces, and c_{ij} are coefficients depending on c_d, c_l and their derivatives with respect to γ, all evaluated at $\bar{\mathcal{C}}$; they are reported in Appendix B.

5. Equilibrium path and stability

Consider the cable in the equilibrium reference configuration $\bar{\mathcal{C}}$, in which it is loaded by its own weight $-mg\mathbf{a}_y$, g being the gravity acceleration, and by the steady-state part $\bar{\mathbf{b}}_a(\varphi, U)$ of the aerodynamic force.

Since, by hypothesis, $\bar{\mathscr{C}}$ is planar, equilibrium requires that the resultant force $\bar{\mathbf{b}}(\varphi, U) := \bar{\mathbf{b}}_a(\varphi, U) - mg\mathbf{a}_y$ lies in the plane of the cable. By enforcing the condition $\bar{\mathbf{b}}(\varphi, U) \cdot \bar{\mathbf{a}}_3 = 0$ (vanishing of the force component along the binormal direction), we obtain, since $\mathbf{a}_y \cdot \bar{\mathbf{a}}_3 = -\sin\varphi$,

$$\sin\varphi = -\frac{\bar{b}_{a_3}(\varphi, U)}{mg}.$$

This equation implicitly defines the nonlinear, nontrivial equilibrium path $\varphi = \varphi(U)$.

The stability of the equilibrium of a generic point of this path is governed by the incremental equations of motion linearized around the reference configuration, namely (16), together with the relevant boundary conditions. Taking into account (18) and (19) for the tangential displacement and twist angle, and (25) for the aerodynamic forces, the problem becomes

$$\bar{T}v'' - EA\frac{\bar{\kappa}^2}{\ell}\int_0^\ell v\,ds + c_{2\vartheta}\vartheta + \hat{c}_{2v}\dot{v} + c_{2w}\dot{w} = m\ddot{v},$$

$$\bar{T}w'' + c_{3\vartheta}\vartheta + c_{3v}\dot{v} + \hat{c}_{3w}\dot{w} = m\ddot{w},$$

$$\vartheta(s,t) = -\frac{GJ + EI}{\sqrt{GJ\,EI}}\int_0^s w''(\xi, t)\sinh\big(k(s-\xi)\big)d\xi + A\cosh ks + B\sinh ks, \tag{26}$$

$$v = 0, \quad w = 0, \quad \vartheta' + \bar{\kappa}w' = 0 \qquad \text{at } s = 0, \ell,$$

where the coefficients $\hat{c}_{2v}$ and $\hat{c}_{3w}$ include structural damping (see Appendix B). All the coefficients c_{ij} depend on the wind velocity. Equations (26) represent a linear eigenvalue problem, of non-self-adjoint type, due to the presence of dissipative (velocity-dependent) and circulatory (position-dependent) forces. It admits infinite solutions of type $v(s,t) = \hat{v}(s)e^{i\lambda t}$, $w(s,t) = \hat{w}(s)e^{i\lambda t}$, where the eigenvalues λ depend on the velocity U. For small U we have $\text{Re}\,\lambda < 0$ for any λ, so $\bar{\mathscr{C}}$ is a stable equilibrium configuration. At a critical wind velocity U_c, however, the couple of complex conjugate eigenvalues having maximum real part crosses the imaginary axes: $\max\text{Re}\,\lambda = 0$. This circumstance causes loss of stability of the equilibrium through a Hopf bifurcation, from which a limit cycle arises, of stable (supercritical, $U \geq U_c$) or unstable (undercritical, $U \leq U_c$) kind.

To solve the boundary value problem (26) we follow a Galerkin approach, in which the in-plane (ϕ_{v_j}) and out-of-plane ($\phi_{w_k}, \phi_{\vartheta_k}$) eigenfunctions of the associated Hamiltonian problem ($c_{ij} = 0$) are taken as trial functions:

$$\begin{pmatrix} \vartheta(s,t) \\ v(s,t) \\ w(s,t) \end{pmatrix} = \sum_{j=1}^m \begin{pmatrix} 0 \\ \phi_{v_j} \\ 0 \end{pmatrix} q_j^i + \sum_{k=1}^n \begin{pmatrix} \phi_{\theta_k} \\ 0 \\ \phi_{w_k} \end{pmatrix} q_k^o, \tag{27}$$

where q_j^i, $j = 1, \ldots, m$, are the unknown amplitudes for the in-plane trial functions and q_k^o, $k = 1, \ldots, n$, are the unknown amplitudes for the out-plane trial functions. By using standard methods, we obtain the *algebraic* eigenvalue problem

$$\mathbf{M}\ddot{\mathbf{q}} + \mathbf{C}\dot{\mathbf{q}} + (\mathbf{K} + \mathbf{H})\mathbf{q} = 0, \tag{28}$$

where $\mathbf{q} = (q_j^i, q_k^o)$ is the $m + n$-vector of the Lagrangian parameters, and $\mathbf{M}$, $\mathbf{C}$, $\mathbf{K}$ and $\mathbf{H}$ are the mass, damping (structural plus aerodynamic), stiffness and circulatory matrices, respectively. These are found

to be block-diagonal, due to symmetric-antisymmetric character of the eigenfunctions. Their coefficients are reported in Appendix C for $m = n = 1$.

6. Numerical results

A numerical analysis has been performed on a sample cable, already analyzed in the literature [Luongo and Piccardo 1998; Yu et al. 1993a; 1993b], having an axial stiffness $EA = 29.7 \times 10^6$ N, a torsional stiffness $GJ = 159$ Nm^2, a diameter $D = 0.0281$ m, a length $\ell = 267$ m, a sag $d = 6.18$ m and damping ratio coefficients equal to 0.44%; moreover, a bending stiffness $EI = 2100$ Nm^2 has been assumed, consistently with experimental observations on several types of cables with sufficiently high axial tension and small curvature values [Hong et al. 2005]. According to these values, the cable is initially close to the first cross-over point [Irvine and Caughey 1984]. The squared ratio between the transversal frequency ω_v and the torsional frequency ω_ϑ (evaluated for the string and the shaft, respectively), is

$$\left(\frac{\omega_v}{\omega_\vartheta}\right)^2 = \frac{\bar{T}}{GJ}\frac{\mathscr{I}_1}{m} \simeq 1.5 \cdot 10^{-2},$$

thus justifying the assumption of quasisteady twisting.

6.1. _Model validation._ A preliminary investigation has been conducted to validate the model. First, the results furnished by the reduced equations of motion (16) and by the complete equations (7) have been compared, in order to numerically check the accuracy of the approximation introduced. A finite-difference analysis has been performed by the algorithm bvp4c in MATLAB to evaluate: (a) the static response of the cable to uniformly distributed forces acting orthogonally to the planar configuration $\mathscr{C}_0$ (Figure 2, left) and, (b) the modal shape assumed by the cable in its first and second out-of-plane normal modes. The results in terms of displacements w, twist ϑ and out-of-plane bending κ_2 are displayed in Figure 3 for static analysis and Figure 4 for dynamic analysis.

Very small differences are furnished by the two models almost everywhere, except for the bending close to the constraints, where, as already noted, the boundary layer is lost using the simplified model. The frequencies computed by both complete and reduced model are $\omega_1 = 1.40$ rad/s, $\omega_2 = 2.80$ rad/s, with differences lower than 0.2%.

The question raised about the non-self-adjointness of the reduced elastic operator was then addressed. It entails that, while out-of-plane displacements w trigger twist rotations ϑ, on the contrary the latter do not force the former. The missing term, believed small, was then reintroduced into the reduced equation, and a static torque applied at one end of the cable, in order to observe out-of-plane displacements. These, however, turned out to be very small, namely $w_{\max}/(\vartheta_{\max}d) = 8 \cdot 10^{-9}$, confirming the accuracy of the reduced model. It is interesting to observe that, in this problem, the bending moment M_2 equilibrating the derivative of the torque M_1' (Equation (5)$_4$) is almost completely induced by the twist angle ϑ, namely $M_2 \simeq EI\bar{\kappa}\vartheta$ (Equations (6)$_3$ and (3)$_2$), that is, the cable remains planar.

Finally, the Galerkin approach (Equations (27)–(28)) has been tested in the evaluation of the critical wind velocity and corresponding critical mode. The exact solution, carried out by the finite-difference analysis, and the approximate solution, obtained by using just one test function for in-plane and out-of-plane motions ($m = n = 1$), have been compared for the sample cable CS2 described further on (with $d = 3$ m and structural damping equal to 0.44%). The first critical velocity is practically coincident in the
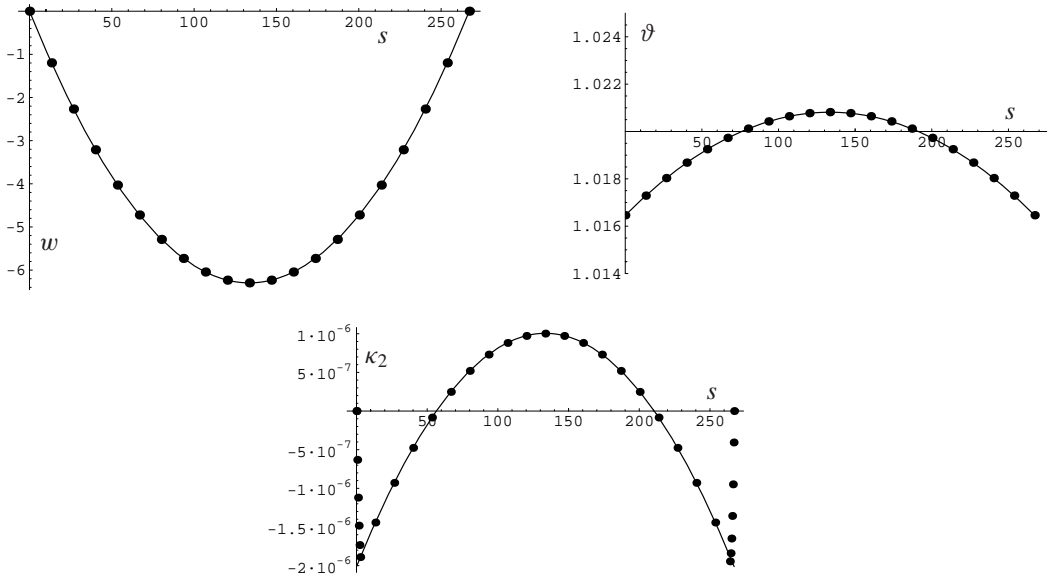
Figure 3. Static response to uniformly distributed forces (dots: complete model; continuous line: reduced model).

two different approaches (about 6.2 m/s). Figure 5 highlights the excellent agreement between critical modes obtained from complete and reduced models: the small differences in the twist angle may be put down to static condensation.

6.2. *Parametric analysis.* A parametric analysis has been conducted to detect the condition of the incipient galloping of cables. Two different U-shaped conductors have been taken into account, already considered in the literature: a cross-section with the symmetry axis placed on $\mathbf{a}_z$-direction (CS1 in the sequel), having its maximum ice eccentricity opposite to the mean wind ($m = 1.80$ kg/m, ice included; see [Yu et al. 1993b]), and a cross-section with the symmetry axis rotated through $-44.4°$ with respect to $\mathbf{a}_z$-direction (CS2 in the sequel), having greater ice thickness ($m = 2.00$ kg/m, ice included; see [Tunstall 1989]). In both cases the specified configuration is the most prone to galloping. It should be noted that, in the proposed theory, this position corresponds to no-wind conditions since the angle of attack γ is also statically varying through the angle of rotation φ; see Equation (23). Therefore, when galloping actually occurs, the cable cross-section is rotated from the more dangerous initial position.

At the lower level, the displacement field $v(s, t)$, $w(s, t)$ and $\vartheta(s, t)$ are approximated by the first symmetric in-plane $\phi_v(s)$ and out-of-plane ($\phi_w(s)$, $\phi_\vartheta(s)$) eigenfunctions of the corresponding Hamiltonian system. Figure 6 shows the nonlinear equilibrium path $\varphi = \varphi(U)$ for the two different cross-sections in the basic case, and the changes in the prestress $\bar{T}$ due to the static loads. Differences are due to aerodynamic coefficients and to cable mass. When the mean wind velocity increases, the rotation soon achieves relevant values and the prestress is subjected to nonnegligible alterations. The conditions of incipient instability are examined by evaluating the real part of the two couples of complex conjugate eigenvalues for the discretized system. The objective is to point out the possible role of the dynamic twist angle ϑ (that is, the circulatory matrix $\mathbf{H}$) on the critical wind velocity U_c. For both cross-sections,

Figure 7 shows the real part of the critical eigenvalue considering (continuous lines) or neglecting (dashed lines) the circulatory matrix $\mathbf{H}$. For CS1 (Figure 7, left), the equilibrium configuration $\bar{\mathscr{C}}$ loses stability at the first bifurcation point B_1, then it regains stability at the second bifurcation point B_2. Differences in the two models are small and slight influence occurs on point B_2. Concerning CS2 (Figure 7, right), the circulatory matrix has again quantitatively small influence, but it is decisive to the occurrence or not of both bifurcations.

It was previously found that the dynamic twist ϑ is much higher in symmetric modes than in anti-symmetric ones. In order to quantify these results, the nonzero coefficients h_{12} and h_{22} of the matrix $\mathbf{H}$ obtained by the Galerkin procedure for $m = n = 1$ (Appendix C), and evaluated for symmetric and antisymmetric modes, were compared; see Figure 8. Three values of $d = d_i$ were considered to explore the situation of almost slack ($d_3 = 15$ m) and almost taut ($d_1 = 3$ m) cable, beside the basic case ($d_2 = 6.18$ m), maintaining the original length $\ell = 267$ m. In the range of the examined velocities, concerning the
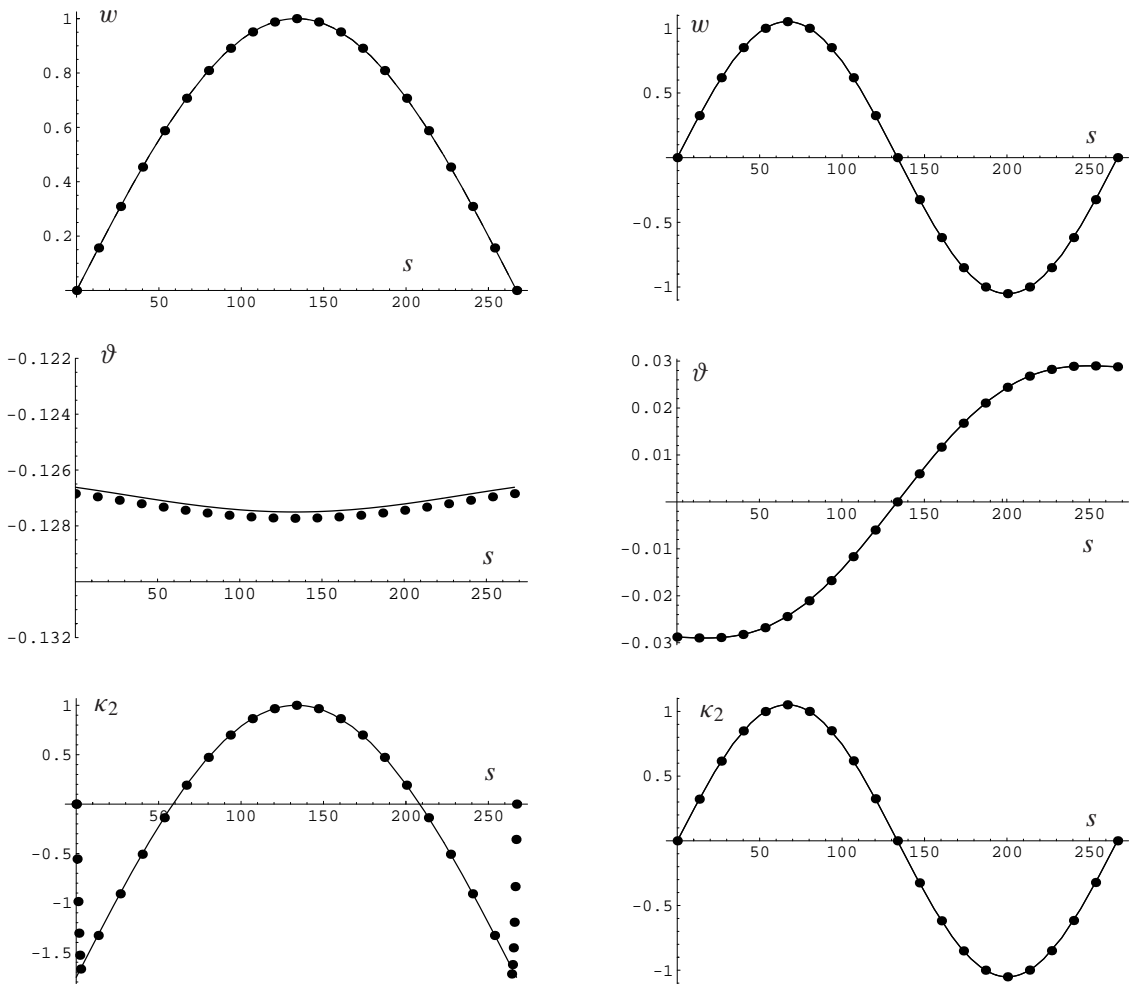

Figure 4. First (left) and second (right) out-of-plane normal mode (dots: complete model; continuous line: reduced model).

antisymmetric modes, the effective influence of the dynamic twist seems to be nonnegligible only for high values of the sag, close to the limits of the proposed theory. By contrast, as regards symmetric modes, the dynamic twist appears remarkable when the curvature (sag) is sufficiently small.

To investigate this aspect with its implications for the system stability, the previous examples related to symmetric modes are reconsidered with suitable changes in mechanical and aerodynamic parameters. Concerning CS1, a reduction of sag and an increase of damping mean that a cable, that is unstable when ignoring the dynamic torsion, is actually stable (Figure 9, left). Moreover, starting the analysis with a cross-section slightly rotated (for example, $-1°$) as regards the position more prone to galloping, the cable cross-section reaches the most dangerous attitude for instability in proximity of the bifurcation points. In this way, bifurcations in both the solutions exist and appreciable differences appear (Figure 9, right).
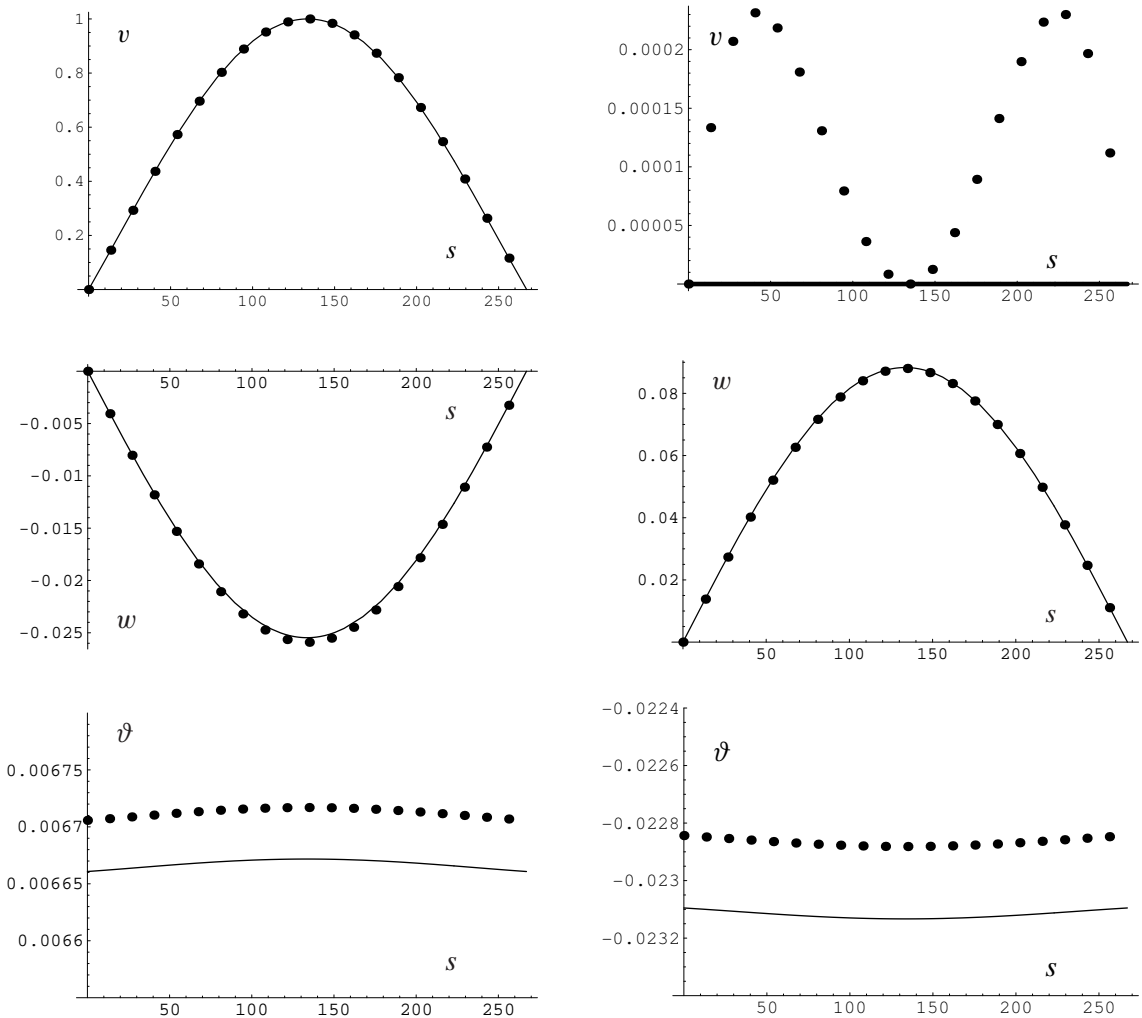

Figure 5. Real (left) and imaginary (right) part of the critical mode (dots: complete model; continuous line: reduced model).
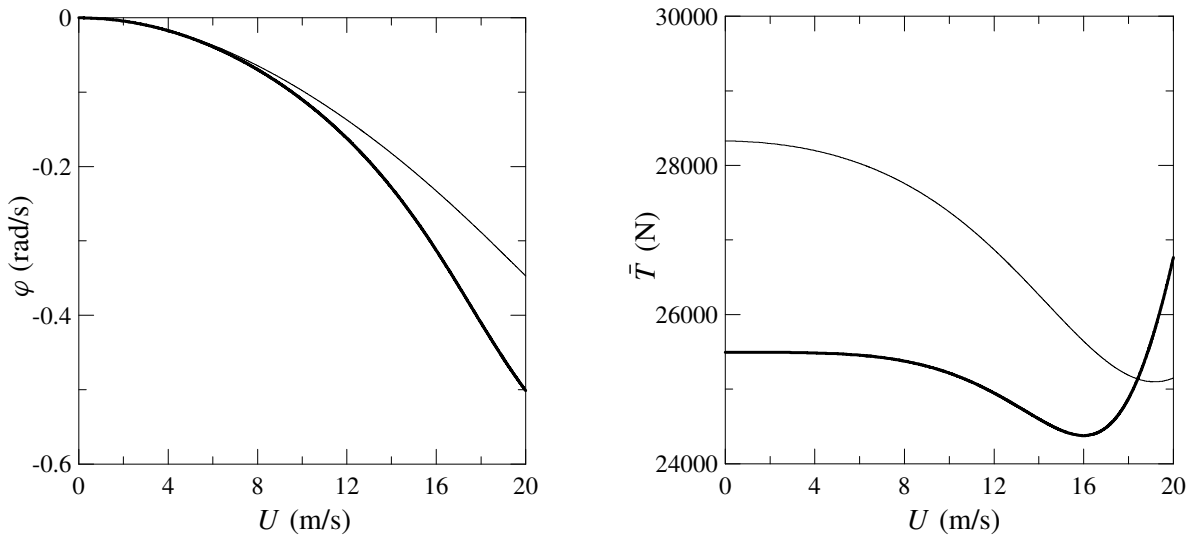
Figure 6. Left: nonlinear equilibrium path $\varphi = \varphi(U)$ for the two different cross-sections in the basic case (thick lines: CS1; thin lines: CS2). Right: changes in the prestress $\bar{T}$ due to the static loads.
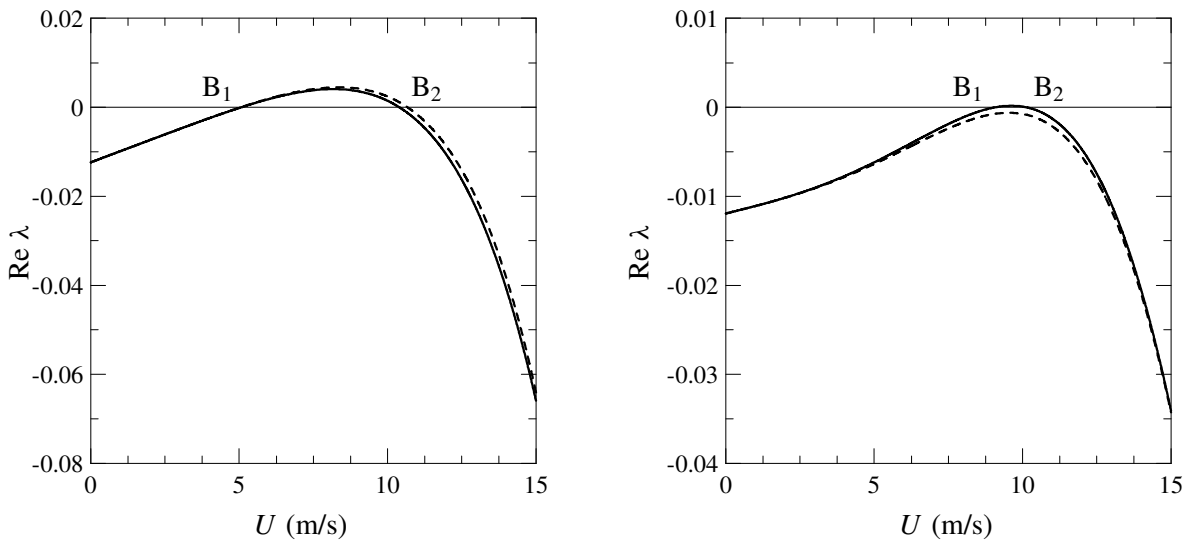

Figure 7. Real part of the critical eigenvalue for CS1 (left) and CS2 (right). Thick lines are used for results obtained with the complete model; dashed lines, for those obtained neglecting the circulatory matrix **H**.

Even larger alteration can be obtained with further increases in the damping ratio. In these latest examples, the contribution of dynamic torsion improves the system stability, but this condition does not appear as a general rule. The influence of dynamic torsion is still more pronounced on the CS2. Maintaining the basic sag and considering an initial rotation of the cross-section equal to $-47°$ (instead of the basic value
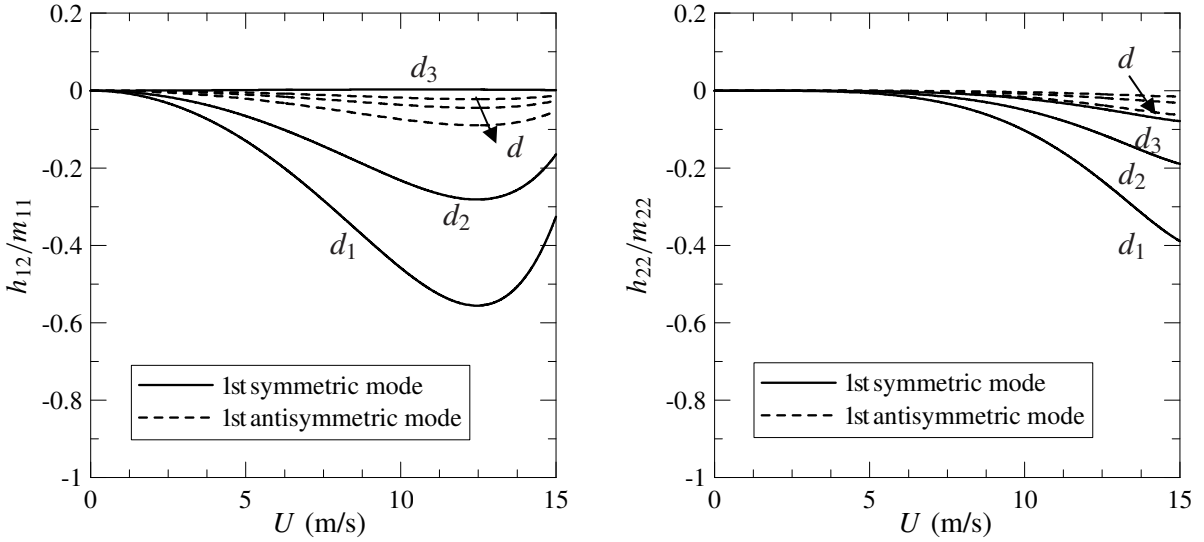
Figure 8. Coefficients of the circulatory matrix **H**: left, coupling terms; right, terms modifying the structural stiffness ($d_1 = 3$ m; $d_2 = 6.18$ m; $d_3 = 15$ m; $\ell = 267$ m; CS1).
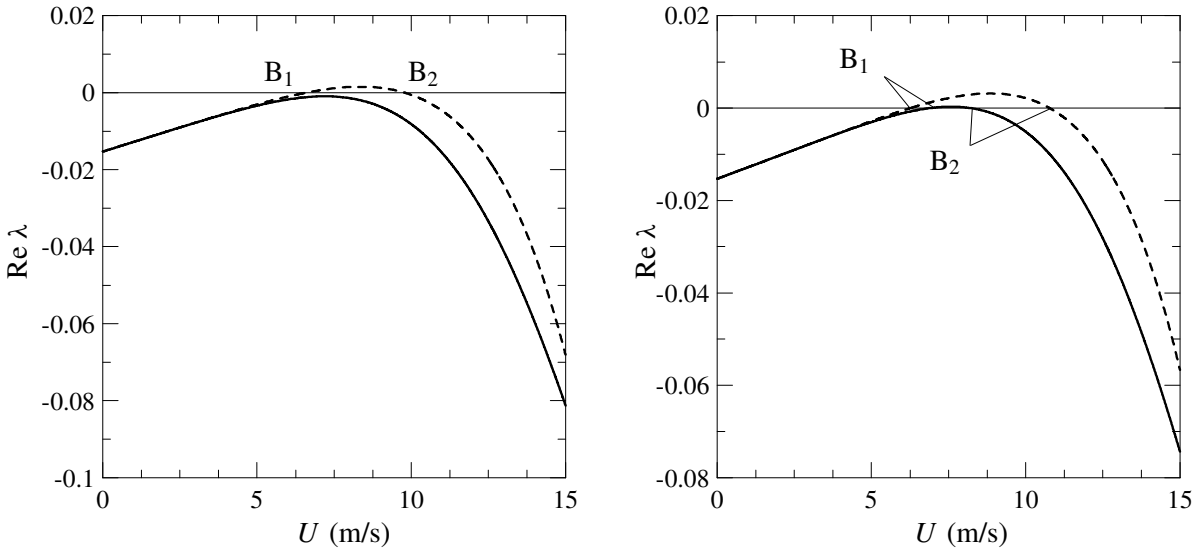

Figure 9. Real part of the critical eigenvalue of the CS1: left, $d = 3$ m; right, $d = 3$ m and sectional symmetry axis rotated through $-1°$ in no-wind conditions (damping coefficients equal to 0.65%). Continuous lines, complete model; dashed lines, matrix **H** neglected.

of $-44.4°$) differences between the two bifurcation points are found immediately (Figure 10, left). If the role of the torsion is exalted by decreasing the sag (Figure 10, right), large alterations of the critical wind velocities appear.
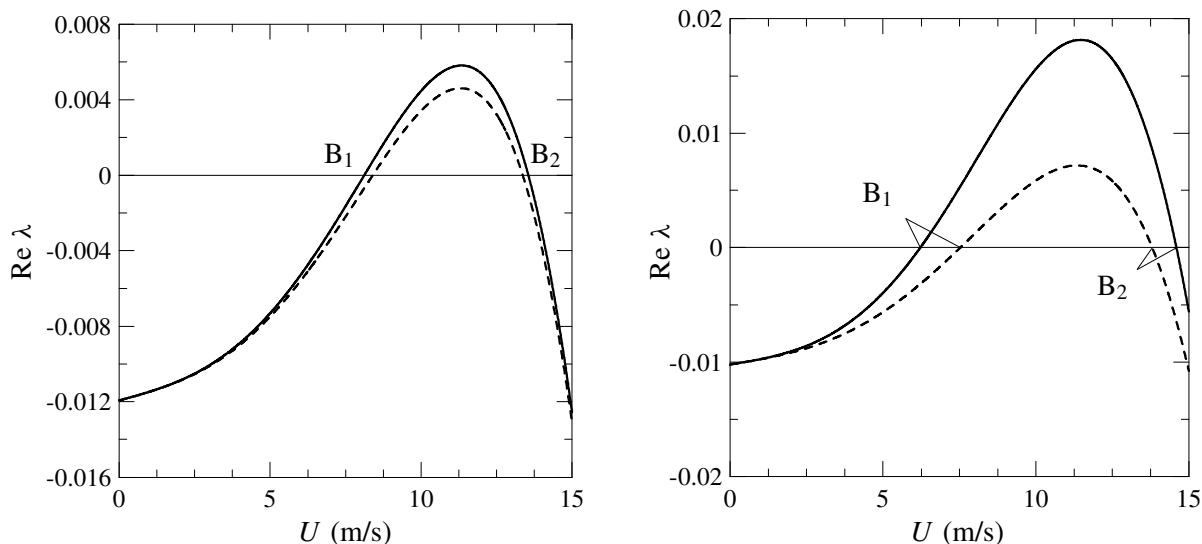
Figure 10. Real part of the critical eigenvalue of the CS2: left, $d = 6.18$ m; right, $d = 3$ m (sectional symmetry axis rotated through $-47°$ in no-wind conditions). Continuous lines, complete model; dashed lines, matrix **H** neglected.

Repeating previous investigations of stability of the antisymmetric modes, qualitatively similar behavior has been obtained, with critical wind velocities equal to, smaller or greater than the critical velocities of symmetric modes. Sometimes, antisymmetric modes always turned out to be stable, since the relevant eigenvalues approach the imaginary axis and then veer away without crossing it. Most importantly, in all the examples considered (not reported here for brevity), the influence of dynamic twist ϑ on the system stability resulted negligible, according to previous theoretical findings.

7. Conclusions

The aim of this paper concerns the formulation of a consistent cable-beam model able to take into account twist angle effects, which can be very important in determining the aeroelastic behavior of these kinds of structure. Several points are worth highlighting.

A consistent model of a linear, curved, prestressed, no-shear, elastic cable-beam has been formulated. Reduced equations of motion have been deduced through a suitable magnitude order analysis; this has made it possible to clarify the different role of the dynamic twist angle on symmetrical and antisymmetrical modes. As a major result, the reduced equations of motion are identical to those of a flexible cable, with an additional equation in the twist angle, which therefore represents a passive variable. The aerodynamic forces have been evaluated taking into account both the angle of static rotation induced by the mean wind and the dynamic twist angle.

Numerical results have been obtained using a Galerkin procedure with translational and twist eigenfunctions, in order to study conditions of incipient instability. It has been proved that the dynamic twist angle is able to influence the critical conditions of the system considerably, through the circulatory matrix, when symmetrical modes are taken into account, especially for small values of sag. The presence of twist

angle may imply the appearance or disappearance of criticality, and may lead to remarkable differences in aeroelastic critical velocities. These alterations are more pronounced when a cross-section is considered in an initially nonsymmetric position.

Appendix A. Magnitude order of the twist angle

The linearized nondimensional equation (11)$_4$ is considered, in which $c_{a_1} = 0$, $\kappa = $ const and $\beta = 1$ are assumed. Moreover,

$$w = \begin{cases} \cos(n\pi s) & n = 1, 3, \ldots \\ \sin(n\pi s) & n = 2, 4, \ldots \end{cases} \qquad s \in \left[-\tfrac{1}{2}, \tfrac{1}{2}\right] \tag{29}$$

is taken, for symmetric and antisymmetric modes, respectively. The equation admits the following approximate solution:

$$\vartheta \simeq \begin{cases} A - 2\kappa \cos(n\pi s) & n = 1, 3, \ldots, \\ B\kappa s - 2\kappa \sin(n\pi s) & n = 2, 4, \ldots, \end{cases}$$

since $\kappa \ll 1$ and therefore $\cosh \kappa s \simeq 1$ and $\sinh \kappa s \simeq \kappa s$ in the interval of interest. By requiring $\vartheta' + \kappa w' = 0$ at $s = \pm 1/2$, the arbitrary constants are found to be $A = \pm 2n\pi/\kappa$, $B = \pm n\pi$, from which, since $\kappa \simeq \delta$ and for n small:

$$\frac{\vartheta}{w} = \begin{cases} \mathbb{O}\left(\tfrac{1}{\delta}\right) & n = 1, 3, \ldots \\ \mathbb{O}(\delta) & n = 2, 4, \ldots \end{cases} \tag{30}$$

Using (30), the first and second derivatives of ϑ are found as in (15), both for symmetric and antisymmetric modes. By summarizing, since the symmetric mode is slow-varying in space, in order to satisfy boundary conditions amplitude A must be large; on the other hand, since the antisymmetric mode is fast-varying in space, amplitude B must, on the contrary, be small.

Appendix B. Static wind forces and aerodynamic coefficients

The static wind force components $\bar{b}_{a_i}$ and the coefficients c_{ij} expressing the dynamic wind force components $b_{a_i} - \bar{b}_{a_i}$, all appearing in Equations (25), are

$$\bar{b}_{a_2} = \tfrac{1}{2}\rho_a U^2 r \left(-c_l \cos \varphi + c_d \sin \varphi\right),$$

$$c_{2\vartheta} = \tfrac{1}{2}\rho_a U^2 r \left(c_l' \cos \varphi - c_d' \sin \varphi\right),$$

$$c_{2v} = \tfrac{1}{4}\rho_a U r \left(-3c_d - c_l' + (c_d - c_l') \cos 2\varphi + (c_d' + c_l) \sin 2\varphi\right),$$

$$c_{2w} = \tfrac{1}{4}\rho_a U r \left(-c_d' + 3c_l + (c_d' + c_l) \cos 2\varphi - (c_d - c_l') \sin 2\varphi\right),$$

$$\bar{b}_{a_3} = \tfrac{1}{2}\rho_a U^2 r \left(c_d \cos \varphi + c_l \sin \varphi\right),$$

$$c_{3\vartheta} = -\tfrac{1}{2}\rho_a U^2 r \left(c_d' \cos \varphi + c_l' \sin \varphi\right),$$

$$c_{3v} = -\tfrac{1}{4}\rho_a U r \left(-c_d' + 3c_l - (c_d' + c_l) \cos 2\varphi + (c_d - c_l') \sin 2\varphi\right),$$

$$c_{3w} = -\tfrac{1}{4}\rho_a U r \left(3c_d + c_l' + (c_d - c_l') \cos 2\varphi + (c_d' + c_l) \sin 2\varphi\right).$$

To include structural damping, the coefficients c_{2v} and c_{3w} are then modified:

$$\hat{c}_{2v} = c_{2v} + c_v, \quad \hat{c}_{3w} = c_{3w} + c_w.$$

Appendix C. Coefficients of the algebraic eigenvalue problem

When $m = n = 1$ in the algebraic problem (28), the Langrangian parameters vector is $\mathbf{q} = (q_1^i, q_1^o)$. The mass matrix is

$$\mathbf{M} = \begin{bmatrix} m_{11} & 0 \\ 0 & m_{22} \end{bmatrix},$$

where

$$m_{11} = -m \int_0^\ell \phi_{v_1}^2 \, ds, \qquad m_{22} = -m \int_0^\ell \phi_{w_1}^2 \, ds.$$

The structural stiffness matrix is

$$\mathbf{K} = \begin{bmatrix} k_{11} & 0 \\ 0 & k_{22} \end{bmatrix},$$

where

$$k_{11} = \bar{T} \int_0^\ell \phi_{v_1} \phi_{v_1}'' \, ds - \frac{EA\bar{\kappa}^2}{\ell} \int_0^\ell \left[\int_0^\ell \phi_{v_1} \, ds \right] \phi_{v_1} \, ds, \quad k_{22} = \bar{T} \int_0^\ell \phi_{w_1} \phi_{w_1}'' \, ds.$$

The circulatory matrix is

$$\mathbf{H} = \begin{bmatrix} 0 & h_{12} \\ 0 & h_{22} \end{bmatrix},$$

where

$$h_{12} = c_{2\vartheta} \int_0^\ell \phi_{v_1} \phi_{\theta_1} \, ds, \qquad h_{22} = c_{3\vartheta} \int_0^\ell \phi_{w_1} \phi_{\theta_1} \, ds$$

The damping matrix $\mathbf{C}$, containing both structural and aerodynamic damping, is

$$\mathbf{C} = \begin{bmatrix} c_{11} & c_{12} \\ c_{21} & c_{22} \end{bmatrix}, \tag{31}$$

where

$$c_{11} = \hat{c}_{2v} \int_0^\ell \phi_{v_1}^2 \, ds, \quad c_{21} = c_{3v} \int_0^\ell \phi_{v_1} \phi_{w_1} \, ds, \quad c_{12} = c_{2w} \int_0^\ell \phi_{v_1} \phi_{w_1} \, ds, \quad c_{22} = \hat{c}_{3w} \int_0^\ell \phi_{w_1}^2 \, ds.$$

In particular, structural damping is introduced directly as modal damping:

$$c_{11} = c_{2v} \int_0^\ell \phi_{v_1}^2 \, ds + 2\xi_1 \sqrt{m_{11}k_{11}}, \quad c_{22} = c_{3w} \int_0^\ell \phi_{w_1}^2 \, ds + 2\xi_2 \sqrt{m_{22}k_{22}},$$

where ξ_1, ξ_2 are the modal damping factors.

References

[Blevins 1990] R. D. Blevins, *Flow-induced vibration*, 2nd ed., Van Nostrand Reinhold, New York, 1990. Reprinted Krieger, Melbourne (FL), 2001.

[Diana et al. 1998] G. Diana, S. Bruni, F. Cheli, F. Fossati, and A. Manenti, "Dynamic analysis of the transmission line crossing 'Lago de Maracaibo' ", *J. Wind Eng. Ind. Aerod.* **74-76** (1998), 977–986.

[Hong et al. 2005] K. J. Hong, A. D. Kiureghian, and J. L. Sackman, "Bending behavior of helically wrapped cables", *J. Eng. Mech. (ASCE)* **131**:5 (2005), 500–511.

[Irvine and Caughey 1984] H. M. Irvine and T. K. Caughey, "The linear theory of free vibrations of a suspended cable", *Proc. R. Soc. London Ser. A* **341** (1984), 299–315.

[Lee and Chao 2000] S. Y. Lee and J. C. Chao, "Out-of-plane vibrations of curved non-uniform beams of constant radius", *J. Sound Vib.* **238**:3 (2000), 443–458.

[Lee and Perkins 1992] C. L. Lee and N. C. Perkins, "Nonlinear oscillations of suspended cables containing a two-to-one internal resonance", *Nonlinear Dynam.* **3**:6 (1992), 465–490.

[Lu and Perkins 1994] C. L. Lu and N. C. Perkins, "Nonlinear spatial equilibria and stability of cables under uni-axial torque and thrust", *J. Applied Mech.* (*ASME*) **61**:4 (1994), 879–886.

[Luongo and Piccardo 1996] A. Luongo and G. Piccardo, "On the influence of the torsional stiffness on non-linear galloping of suspended cables", pp. 273–276 in *Proc. 2nd European Nonlinear Oscillations Conference* (Prague, 1996), Ústav termo-mechaniky, Akademie věd ČR, Prague, 1996.

[Luongo and Piccardo 1998] A. Luongo and G. Piccardo, "Non-linear galloping of sagged cables in 1:2 internal resonance", *J. Sound Vib.* **214**:5 (1998), 915–940.

[Luongo et al. 1984] A. Luongo, G. Rega, and F. Vestroni, "Planar non-linear free vibrations of an elastic cable", *Int. J. Non-Linear Mech.* **19**:1 (1984), 39–52.

[Luongo et al. 2005] A. Luongo, D. Zulli, and G. Piccardo, "Un modello lineare di trave curva per l'analisi delle oscillazioni galoppanti di cavi sospesi", in *Atti del XVII Congresso Nazionale AIMETA* (Florence, 2005), 2005. Available in CD-ROM.

[McConnel and Chang 1986] K. G. McConnel and C. N. Chang, "A study of the axial-torsional coupling effect on a sagged transmission line", *Exp. Mech.* **26**:4 (December 1986), 324–329.

[Strømmen and Hjorth-Hansen 1995] E. Strømmen and E. Hjorth-Hansen, "The buffeting wind loading of structural members at an arbitrary attitude in the flow", *J. Wind Eng. Ind. Aerod.* **56**:2-3 (1995), 267–290.

[Tunstall 1989] M. Tunstall, "Accretion of ice and aerodynamic coefficients", in *Proceedings of the Association des Ingénieurs Montefiore (AIM) Study Day on Galloping* (Liège, 1989), Université de Liège, 1989.

[White et al. 1991] W. N. White, S. Venkatasubramanian, P. M. Lynch, and C. D. Huang, "The equations of motion for the torsional and bending vibrations of a stranded cable", pp. 91–WA/APM–19 in *ASME Winter Annual Meeting*, ASME, New York, 1991.

[Yu et al. 1993a] P. Yu, Y. M. Desai, A. H. Shah, and N. Popplewell, "Three-degree-of-freedom model for galloping, I: formulation", *J. Eng. Mech.* (*ASCE*) **119**:12 (1993), 2404–2425.

[Yu et al. 1993b] P. Yu, Y. M. Desai, A. H. Shah, and N. Popplewell, "Three-degree-of-freedom model for galloping, II: solutions", *J. Eng. Mech.* (*ASCE*) **119**:12 (1993), 2426–2448.

ANGELO LUONGO: luongo@ing.univaq.it
DISAT, Università degli Studi di L'Aquila, 67040 L'Aquila (AQ), Italy

DANIELE ZULLI: danzulli@ing.univaq.it
DISAT, Università degli Studi di L'Aquila, 67040 L'Aquila (AQ), Italy

GIUSEPPE PICCARDO: giuseppe.piccardo@unige.it
DICAT, Università degli Studi di Genova, Via Montallegro, 1, 16145 Genova (GE), Italy